Vol 18 No 4, April 2009
1674-1056/2009/18(04)/1627-04

Chinese Physics B

© 2009 Chin. Phys. Soc.
and IOP Publishing Ltd

Numerical model of multilayer organic light-emitting devices*

Hu Yue(胡 玥) and Rao Hai-Bo(饶海波)†

School of Optoelectronic Information, University of Electronic Science and Technology of China (UESTC), Chengdu 610054, China

(Received 1 September 2008; revised manuscript received 28 November 2008)

A numerical model of multilayer organic light-emitting devices is presented in this article. This model is based on the drift-diffusion equations which include charge injection, transport, space charge effects, trapping, heterojunction interface and recombination process. The device structure in the simulation is ITO/CuPc (20 nm)/NPD (40 nm)/Alq3 (60 nm)/LiF/Al. There are two heterojunctions which should be dealt with in the simulation. The I–V characteristics, carrier distribution and recombination rate of a device are calculated. The simulation results and measured data are in good agreement.

Keywords: organic light-emitting devices, multilayer, simulation
PACC: 7360R, 7210B, 7120H

1. Introduction

Organic light-emitting devices (OLEDs) have attracted a lot of attention ever since the discovery of low operation voltage OLED.[1−4] OLEDs have the potential to revolutionalize display technology by relying on their own unique features, such as low power consumption, high brightness, high contrast, and potentially low-cost high performance self-emissive display.

Although OLEDs have been studied in the last decade, there is still much room for further understanding of the fundamental device physics and for improving the device performances. It is important to develop a device model to help optimize the device parameters. Many models have been studied for single layer OLEDs and multilayer OLEDs.[4−8] In the present article, a numerical model of multilayer organic light-emitting device is presented.

2. Model

The carrier transport model of the organic device is described by drift–diffusion equations of current density coupled to the Poisson equation as follows:[9]

$$\frac{\mathrm{d}J_n}{\mathrm{d}x} = q(R-G), \tag{1}$$

$$\frac{\mathrm{d}J_p}{\mathrm{d}x} = -q(R-G), \tag{2}$$

$$\frac{\mathrm{d}}{\mathrm{d}x}\left(\varepsilon_0\varepsilon_\mathrm{r}\frac{\mathrm{d}\psi}{\mathrm{d}x}\right) = -q(p-n-n_\mathrm{t}+p_\mathrm{t}), \tag{3}$$

where J_n and J_p are the electron and the hole current densities respectively; q is the electron charge; R is the recombination rate; G is the generation rate expressed as $G = \dfrac{q(\mu_n+\mu_p)}{\varepsilon_0\varepsilon_\mathrm{r}}(n_e p_e)$, with n_e and p_e being electron and hole equilibrium densities, respectively; n and p are the densities of free electrons and holes, respectively; ψ is the electrostatic potential; $\varepsilon_0\varepsilon_\mathrm{r}$ is the permittivity of the organic material; n_t and p_t are the densities of trapped electrons and holes of the organic material; μ_n and μ_p are carrier mobilities, which are expected to be field dependent in the amorphous organic materials and given by Poole–Frenkel form[10,11]

$$\mu = \mu_0 \exp(\sqrt{E/E_0}) \tag{4}$$

with μ_0 being the zero-field mobility, E the electric field, and E_0 the field-dependent parameter (material parameter). In an organic material with an energy gap larger than 2 eV, carrier generation is very small so that it can be neglected.

The Maxwell–Boltzmann statistics is assumed, so the electron and the hole concentrations are expressed

*Project supported by Zhejiang Yangguang Cooperation Foundation, China (Grant No W050317).
†E-mail: rhb@uestc.edu.cn

as

$$n = N_{\mathrm{LUMO}} \exp\left(\frac{F_n - E_{\mathrm{LUMO}}}{kT}\right), \quad (5)$$

$$p = N_{\mathrm{HOMO}} \exp\left(\frac{E_{\mathrm{HOMO}} - F_p}{kT}\right), \quad (6)$$

where k is Boltzmann's constant; T is the device temperature; F_p and F_n are quasi-Fermi levels for electrons and holes; E_{LUMO} and E_{HOMO} are energy levels of the lowest unoccupied molecular orbital (LUMO) and the highest occupied molecular orbital (HOMO); N_{LUMO} and N_{HOMO} are the densities of the states of the carrier in LUMO and HOMO, respectively. ($N_{\mathrm{LUMO}} = N_{\mathrm{HOMO}} = 10^{20}\,\mathrm{cm}^{-3}$).

An exponential distribution form is used for electron trap density of the host and given as

$$n_{\mathrm{t}}(E) = \left(\frac{N_{\mathrm{t}}}{kT_{\mathrm{t}}}\right) \exp\left(\frac{E - E_{\mathrm{LUMO}}}{kT_{\mathrm{t}}}\right), \quad (7)$$

where $n_{\mathrm{t}}(E)$ is the trap density at energy E, N_{t} is the total density of traps, and T_{t} is the characteristic temperature of the exponential trap distribution. The hole trap density has a similar form.

The recombination rate of free carrier is given by the Langevin form[12] as

$$R = \frac{q}{\varepsilon_0 \varepsilon_{\mathrm{r}}}(\mu_n + \mu_p)(np). \quad (8)$$

In this simulation the charge injection barrier (Schottky barrier Ψ_{b}) at the electrodes can be considered to have the work function ϕ_{M} for each metal electrode. The surface potential Ψ_{s} at a Schottky contact is defined as

$$\psi_{\mathrm{s}} = \chi_{\mathrm{c}} + \frac{E_{\mathrm{g}}}{2q} + \frac{kT}{2q} In \frac{N_{\mathrm{LUMO}}}{N_{\mathrm{HOMO}}} - \phi_{\mathrm{m}} + V_{\mathrm{app}}, \quad (9)$$

where the electron affinity of the semiconductor is related to the Schottky barrier height and the metal work function by $\phi_{\mathrm{m}} = \Psi_{\mathrm{b}} + \chi_{\mathrm{C}}$.

The boundary conditions are given by specifying the particle currents at the boundaries $x = 0$ and $x = L$. There are three particle current components, i.e. thermionic emission, a backflowing interface recombination current that is the time reversed process of thermionic emission, and tunnelling.[6] The Fowler–Nordheim (F–N) injection for the tunnelling contact is used.

Equations (1)–(3) are solved numerically. The Scharfetter–Gummel[13] approach has been utilized to discretize the continuity equations in order to obtain the numerical solution.

Energy level discontinuities at the organic heterojunction are also considered in the present work.[8]

The position independence of the total current $J = J_n + J_p$ is used to verify that steady-state has been reached.

3. Simulation results

Simulation results are presented for a multilayer structure consisting of ITO/CuPc/NPD/Alq_3/LiF/Al. The energy level diagram of the multilayer OLED device is shown in Fig.1. Devices under investigation in this study were prepared by vacuum vapour deposition, with ITO-coated glass used as substrates. The ITO substrates were pretreated with oxygen plasma prior to the deposition of organic layers in order to enhance the work function of the ITO. This resulted in better energy level alignment between the ITO work function and the CuPc work function. Voltage-current measurements were performed by using a Keithley 2400 high current source measurement unit.

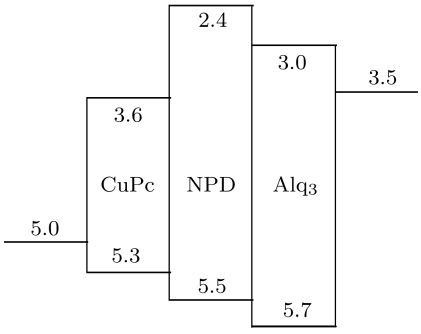


Fig.1. Energy level diagram for the multilayer device.

The mobility parameters used in the simulation are shown in Table 1. The carrier distribution on a multilayer device was simulated for the case where an applied bias was at 6 V. The electron and the hole distribution are shown in Fig.2. Electrons are injected from the cathode and holes from the anode. There appears an accumulation of holes at the two heterojunctions (20 nm and 60 nm). There is also accumulation of electrons at the interface between NPD and Alq_3 (60 nm), which is bigger than that of hole. Because the electronic barrier between Alq3 and NPD is 0.6 eV, while the hole barrier between Alq3 and NPD is 0.2 eV. And the electron mobility in NPD is too

Table 1. Mobility parameters.

	$\mu_{n0}/(\mathrm{cm}^2/\mathrm{Vs})$	$E_{n0}/(\mathrm{V/cm})$	$\mu_{p0}/(\mathrm{cm}^2/\mathrm{Vs})$	$E_{p0}/(\mathrm{V/cm})$
CuPc	6.9×10^{-5}	1.686×10^{4}	1.0×10^{-6}	1.235×10^{4}
NPD	1.0×10^{-6}	1.111×10^{5}	1.8×10^{-5}	7.716×10^{4}
Alq_3	8.0×10^{-8}	1.085×10^{4}	7.0×10^{-10}	1.235×10^{4}

small, it is difficult for electrons to drift and diffuse in NPD. Figure 3 shows the recombination rate in the device. The rate is biggest in the interface between Alq3 and NPD as the hole and electron mobilities are both biggest in this position. The recombination rate in Alq3 is more than two orders of magnitude higher than that in NPD. So Alq3 is a good choice as an emission layer in this structure.

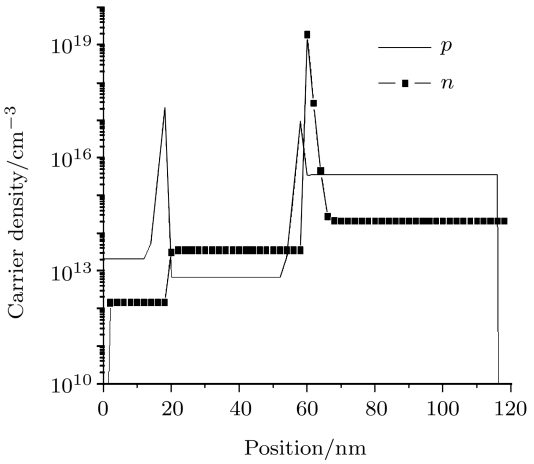


Fig.2. Carrier density distribution in the device at bias = 6 V.

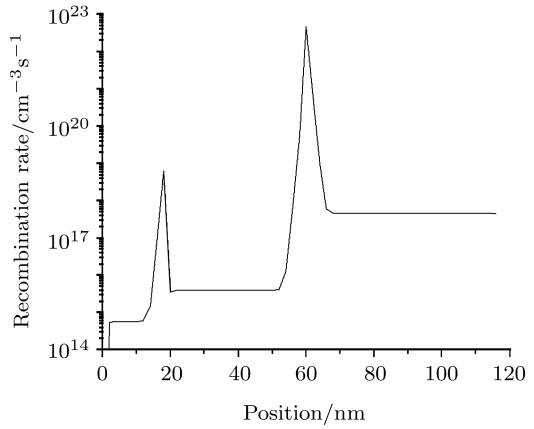


Fig.3. Recombination rate of device at bias = 6 V.

Figure 4 indicates a comparison of I–V characteristic between simulation and measured data. As can be seen from the figure, the simulation data are in good agreement with the measured data in a large range.

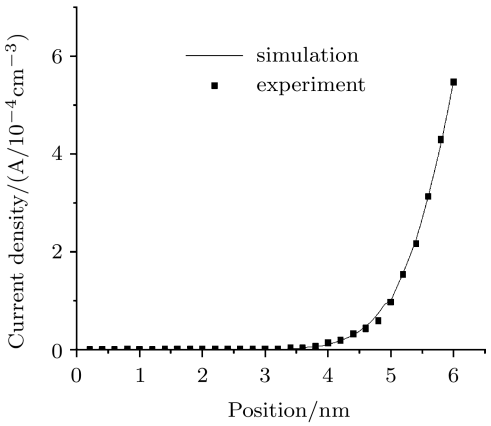


Fig.4. Measured and calculated current densities for a multilayer device.

Electron quasi-Fermi (F_n) and hole quasi-Fermi (F_p) energy distributions can be calculated by using the Maxwell–Boltzmann statistics. Figure 5 shows the LUMO, HOMO, electron quasi-Fermi energy (F_n) and hole quasi-Fermi (F_p) energy at a bias voltage of 7.8 V. From the figure, it can be seen that F_p and F_n are in the gap of the organic material. The Maxwell–Boltzmann statistics can be used here.

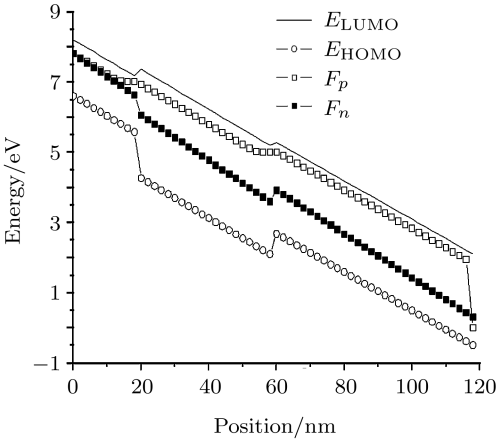


Fig.5. Curves for LUMO, HOMO, electron quasi-Fermi and hole quasi-Fermi energies at bias = 7.8 V.

4. Conclusions

A numerical model for the simulation of multilayer organic light-emitting devices is developed. The carrier injection, the transport process and the recombination process are considered in the simulation. The carrier transport through the heterojunction interface is discussed particularly. The calculation is based on a device with a structure composed of ITO/CuPc(20 nm)/NPD(40 nm)/Alq3(60 nm)/LiF/Al where there are two heterojunction interfaces, which represent the typical device configuration actually accepted in most current OLED research work. The I–V characteristics, the carrier distribution and the recombination rate are calculated. The simulation results and the measured data are in good agreement.

References

[1] Tang C W and VanSlyke S A 1987 *Appl. Phys. Lett.* **51** 913

[2] Konezny S J, Smith D L , Galvin M E and Rothberg L J 2006 *J. Appl. Phys.* **99** 64509

[3] Brütting W, Berleb S and Mückl A 2001 *Org. Electronics.* **2** 1

[4] Scott J C, Carter S A, Karg S and Angelopoulos A 1997 *Synth. Metals* **85** 1197

[5] Hu Y and Rao H B 2008 *Acta Phys. Sin.* **57** 5928 (in Chinese)

[6] Davids P S, Campbell I H and Smith D L 1997 *J. Appl. Phys.* **82** 6319

[7] Campbell I H, Davids P S, Smith D L, Barashkov N N and Ferraris J P 1998 *Appl. Phys. Lett.* **72** 1863

[8] Crone B K, Davids P S, Cambell I H and Smith D L 2000 *J. Appl. Phys.* **87** 1974

[9] Liu E K, Zhu B S and Luo J S 2003 *Physics of Semiconductor* (Beijing: Publishing House of Electronics Industry) (in Chinese)

[10] Malliaras G G, Salem J R, Brock P J and Scott J C 1998 *Phys. Rev.* B **58** R13411

[11] Scott J C, Karg S and Carter S A 1997 *J. Appl. Phys.* **82** 1454

[12] Parker I D 1994 *J. Appl. Phys.* **75** 1656

[13] Scharfetter D L and Gummel H K 1969 *IEEE Transactions on Electron Devices* **16** 64